

“On the Foundation of Transport-Driven Diffusion for Neutron Transport Problems”

*Original*

“On the Foundation of Transport-Driven Diffusion for Neutron Transport Problems” / Picca, Paolo; Furfaro, Roberto; Dulla, Sandra; Ravetto, Piero. - In: JOURNAL OF COMPUTATIONAL AND THEORETICAL TRANSPORT. - ISSN 2332-4325. - 51:5(2022), pp. 305-328. [10.1080/23324309.2022.2110897]

*Availability:*

This version is available at: 11583/2973492 since: 2022-11-30T10:22:30Z

*Publisher:*

TAYLOR & FRANCIS INC

*Published*

DOI:10.1080/23324309.2022.2110897

*Terms of use:*

This article is made available under terms and conditions as specified in the corresponding bibliographic description in the repository

*Publisher copyright*

(Article begins on next page)

Title: “On the foundation of transport-driven diffusion for neutron transport problems”

Authors:

- Paolo Picca (corresponding author), University of Arizona, Department of Systems and Industrial Engineering, P.O. Box 210020 - Tucson, AZ 85721, USA;  
[ppicca@email.arizona.edu](mailto:ppicca@email.arizona.edu)
- Roberto Furfaro, University of Arizona, Department of Systems and Industrial Engineering, P.O. Box 210020 - Tucson, AZ 85721, USA;  
[robertof@email.arizona.edu](mailto:robertof@email.arizona.edu)
- Sandra Dulla, Politecnico di Torino, Dipartimento Energia, NEMO group, Corso Duca degli Abruzzi, 24 - 10129 Torino, Italy  
[Sandra.dulla@polito.it](mailto:Sandra.dulla@polito.it)
- Piero Ravetto, Politecnico di Torino, Dipartimento Energia, NEMO group, Corso Duca degli Abruzzi, 24 - 10129 Torino, Italy  
[Piero.ravetto@formerfaculty.polito.it](mailto:Piero.ravetto@formerfaculty.polito.it)

Figures: 11

Tables: 3

## **ABSTRACT**

The paper presents the foundation of a novel methodology developed for the solution of the neutron transport equation, named the transport driven-diffusion approach, which can be considered as an evolution of the classic multiple collision method. The idea behind this method is based on the expansion of the full solution in terms of the contributions of the particles emitted by successive collisions plus a residual term, accounting for particles which have undergone more than a predefined number of collisions. In order to determine the contribution at each collision order, a transport equation with a source term is solved, while the estimation of the residue is based on a diffusion theory model. The physical rationale for the choice of the diffusion model for the residue is discussed and justified, as physics suggests that the diffusion assumptions become more applicable for the description of the particles having suffered a certain number of collisions rather than to the original transport problem. Some results are presented for a set of steady-state and time-dependent test cases. Their analysis shows the remarkable advantage of the method proposed in terms of accuracy and computational time, when compared to standard diffusion and multiple collision at the same order.

**Keywords:** neutron transport equation, multiple collision method, diffusion theory.

## Dedication

The authors want to dedicate this work to Barry D. Ganapol, to show their deep gratitude for the sincere friendship that has been established with him along many years, for one of them throughout several decades. For all of us Barry has always been much more than just a colleague.

On the human side, he has been a real and generous fraternal friend. We have so many vivid remembrances of the nice time we have spent together in all the occasions we could meet at various conferences around the world and during the several visits of his to Politecnico di Torino. We always had a great convivial time, while talking of almost anything one can think of, exchanging personal experiences or just enjoying. Barry, it has been a great and enriching experience for us to know you and to be able to share some of our time with you.

On the scientific side, he has always been a source of inspiration. We recognize how important his work on transport theory is and how fertile his rigorous analytical approach has turned out to be. A discussion on a scientific matter with him has always been fruitful and he has taught so much to us, disclosing so many subtleties of the Boltzmann equation. Thank you, “transport cow-boy”!

The analysis presented in this paper has been stimulated by the seminal work that Barry has carried out over the years on the multiple collision approach for the solution of the transport equation. We believe it is an appropriate choice to dedicate it to Barry, as the transport process in which particles of a given generation accumulate information on the nature of the system from previous generations can be considered as a metaphor of our scientific lives, as the younger generations have learned from the scientific experiences of the older ones, all the way up to Barry.

With this contribution we want to wish you, Barry, all the best, good health, a good time and further scientific success for long!

חֵן וְכָרוֹךְ

## 1. INTRODUCTION

The simulation of neutral particle transport in a scattering, absorbing and/or multiplying medium is rigorously described by the linear Boltzmann equation (LBE). Due to the integro-differential mathematical nature of the transport equation (Davison, 1957; Case and Zweifel, 1967), its solution in a closed-form is possible only for a very limited number of problems, often of purely academic interest. For real applications, in particular to reactor physics simulations, in the past decades a variety of approximations were devised to reduce the computational burden of the solution of the LBE. For a large class of problems, the diffusion model represents a reasonable approximation of the transport process, which adequately describes the behavior of the bulk of the particle field determined by the collision process (typically far from strong sources and absorbers and from system boundaries). The connection between transport and diffusion models clearly appears from a theoretical point of view. As an example, using the singular eigenfunction expansion method (Case, 1960), it can be shown that the complete solution of the linear transport equation can be written as the sum of a diffusive term and a transport term rapidly decreasing moving away from the source.

For steady-state problems, several approximate methodologies show an inherent connection with diffusion. For example, when using the spherical harmonics expansion method ( $P_N$  method; Meghreblian and Holmes, 1960), the diffusion equation corresponds to the  $P_1$  approximation in a general geometry setup, whereas for the discrete ordinate approach ( $S_N$  method) the  $S_2$  approximation leads to diffusion in one-dimensional slab geometry (Bell and Glasstone, 1970). The diffusion theory can also be derived from the LBE via **asymptotic analysis** for both steady-state and time-dependent transport problems in general multidimensional geometry in case of isotropic emissions (e.g., Larsen, 1980). Additionally, in the past hybrid methodologies were also explored for the solution of the LBE with domain decomposition (e.g., Ball, 2002a; 2002b), combining diffusion solution in diffusive regions (i.e., highly scattering materials in regions far from boundaries) with a transport solution in non-diffusive areas (i.e., “clear” regions). **The idea of using diffusion to accelerate a transport solution has been also adopted in connection with Monte Carlo simulations, by obtaining statistical information**

on the particle behavior through a diffusive solution in specific sub-domains, to accelerate the Monte Carlo sampling (e.g. see an application to radiative transfer in Gentile, 2001).

More recently, a novel solution technique for the LBE was proposed in (Picca and Furfaro, 2014). The so-called transport-driven diffusion (or TDD) is based on heuristic considerations, which recognize that the bulk of the particle field is dominated by a diffusion model describing the contribution of the particles that have suffered a high number of collisions and correct its inaccuracy with a transport description of the particles that have experienced only few collisions. Results show that the intuition is fundamentally correct and the advantage of TDD versus pure diffusion is evident even at low orders (i.e., considering only particles having suffered a low number of collisions). Similarly, a multi-collision scheme was proposed in the past for improving the efficiency of Monte Carlo simulation when dealing with diffusive media (Densmore, 2006).

In addition to the use of a diffusion model to enhance the solution of a transport problem, it is also important to call the attention on a powerful method to accelerate to source iterations process that is widely used in standard deterministic computational tools, i.e. the Diffusion Synthetic Acceleration (DSA), see Adams and Larsen (2002) for a comprehensive review. However, present approach significantly differs from DSA, as:

- DSA is a method for accelerating the original solution of transport equations, while TDD provides a model approximation of the solution of the linear Boltzmann equation;
- DSA couples a diffusion solver to a full transport code (e.g. discrete ordinates), while, as will be shown in this work, the transport-like part of the solution in TDD is obtained by a simple ray tracing for the first collisions contributions, without the need to converge on the collision source.

The motivation of the present paper is to provide a more robust mathematical background to TDD, based on asymptotic analysis. Additionally, the paper also discusses a possible metric to measure the distance from the diffusive regime, which can be helpful in the practical implementation of TDD to set the truncation order (i.e., the transition from transport to diffusion).

The remainder of the paper is organized as follows. The derivation of the diffusion model as a first-order **asymptotic** expansion of the LBE is recalled in Sect. 2 with a review of the basic hypothesis for the scaling used. Section 3 derives the TDD method using the multiple collision approach via **asymptotic analysis**, detailing the critical parameter for the transition from transport to the diffusive behavior. The efficiency and flexibility of TDD are proven considering several test cases in Sect. 4, before drawing some final remarks and suggestions for future work in Sect. 5.

## 2. **ASYMPTOTIC DERIVATION OF THE DIFFUSION MODEL FROM THE LINEAR BOLTZMANN EQUATION**

The time-dependent linear Boltzmann equation for monoenergetic particles of velocity  $v$  in the Cartesian coordinate system with isotropic scattering and source emission is written as (e.g., Davison, 1957; Case and Zweifel, 1967; Bell and Glasstone, 1970):

$$\left[ \frac{1}{v} \frac{\partial}{\partial t} + \boldsymbol{\Omega} \cdot \boldsymbol{\nabla} + \Sigma(\mathbf{r}) \right] \psi(\mathbf{r}, \boldsymbol{\Omega}, t) = \frac{\Sigma_s(\mathbf{r}) + v\Sigma_f(\mathbf{r})}{4\pi} \oint \psi(\mathbf{r}, \boldsymbol{\Omega}', t) d\boldsymbol{\Omega}' + \frac{1}{4\pi} q(\mathbf{r}, t), \quad (1)$$

where  $\psi$  is the angular flux and the other symbols used have their standard meaning. The boundary and initial conditions can generally be written as:

$$\begin{aligned} \psi(\mathbf{r}_s, \boldsymbol{\Omega}, t) &= f(\mathbf{r}_s, \boldsymbol{\Omega}, t) \quad \text{for} \quad \boldsymbol{\Omega} \cdot \mathbf{n}_s < 0, \\ \psi(\mathbf{r}, \boldsymbol{\Omega}, t = 0) &= \psi_0(\mathbf{r}, \boldsymbol{\Omega}), \end{aligned} \quad (2)$$

where  $\mathbf{r}_s$  is the boundary of the system and  $\mathbf{n}_s$  is the outward-oriented unit vector normal to the surface. The function  $f$  defines a given boundary source term.

The diffusion approximation of the linear transport equation can be obtained via **asymptotic analysis** (Larsen, 1980), considering the following scaling in terms of the small parameter  $\varepsilon$ :

$$\frac{1}{v} \rightarrow \frac{\varepsilon}{v}, \quad (3a)$$

$$\Sigma \rightarrow \frac{\Sigma}{\varepsilon}, \quad (3b)$$

$$\Sigma_s \rightarrow \frac{\Sigma}{\varepsilon} - \varepsilon \Sigma_a, \quad (3c)$$

$$v \Sigma_f \rightarrow \varepsilon v \Sigma_f, \quad (3d)$$

$$q \rightarrow \varepsilon q. \quad (3e)$$

The scaling of the velocity as the inverse of  $\varepsilon$  in Eq. (3a) implies a high velocity of particles and hence the perturbation effects are smoothed by the fast propagation of signals. The relations in Eqs. (3b)-(3c) is based on the assumption of a medium characterized by a large collisionality and a low absorption. The scaling of the source in Eq. (3e) implies a small contribution of the external source with respect to the scattering emission term. In this derivation, the fission term is considered to scale with  $\varepsilon$ , as the external source.

The solution of Eq. (1) can be expressed with the following **asymptotic** expansions in the parameter  $\varepsilon$ :

$$\psi(\mathbf{r}, \boldsymbol{\Omega}, t) = \psi_0(\mathbf{r}, \boldsymbol{\Omega}, t) + \varepsilon \psi_1(\mathbf{r}, \boldsymbol{\Omega}, t) + \varepsilon^2 \psi_2(\mathbf{r}, \boldsymbol{\Omega}, t) + \dots = \sum_{n=0}^{\infty} \varepsilon^n \psi_n(\mathbf{r}, \boldsymbol{\Omega}, t), \quad (4a)$$

$$\Psi(\mathbf{r}, t) = \Psi_0(\mathbf{r}, t) + \varepsilon \Psi_1(\mathbf{r}, t) + \varepsilon^2 \Psi_2(\mathbf{r}, t) + \dots = \sum_{n=0}^{\infty} \varepsilon^n \Psi_n(\mathbf{r}, t), \quad (4b)$$

where the scalar flux is defined with

$$\Psi(\mathbf{r}, t) = \oint \psi(\mathbf{r}, \boldsymbol{\Omega}, t) d\boldsymbol{\Omega}.$$

Substituting Eq. (4) into Eq. (1), the following equalities are obtained at the various order of  $\varepsilon$ :

$$\varepsilon^{-1} \rightarrow \psi_0(\mathbf{r}, \boldsymbol{\Omega}, t) = \frac{1}{4\pi} \Psi_0(\mathbf{r}, t), \quad (5a)$$

$$\varepsilon^0 \rightarrow \boldsymbol{\Omega} \cdot \nabla \psi_0(\mathbf{r}, \boldsymbol{\Omega}, t) + \Sigma(\mathbf{r})\psi_1(\mathbf{r}, \boldsymbol{\Omega}, t) = \frac{\Sigma(\mathbf{r})}{4\pi} \Psi_1(\mathbf{r}, t), \quad (5b)$$

$$\begin{aligned} \varepsilon^1 \rightarrow \frac{1}{v} \frac{\partial}{\partial t} \psi_0(\mathbf{r}, \boldsymbol{\Omega}, t) + \boldsymbol{\Omega} \cdot \nabla \psi_1(\mathbf{r}, \boldsymbol{\Omega}, t) + \Sigma(\mathbf{r})\psi_2(\mathbf{r}, \boldsymbol{\Omega}, t) \\ = \frac{v\Sigma_f(\mathbf{r}) - \Sigma_a(\mathbf{r})}{4\pi} \Psi_0(\mathbf{r}, t) + \frac{\Sigma(\mathbf{r})}{4\pi} \Psi_2(\mathbf{r}, t) + \frac{1}{4\pi} q(\mathbf{r}, t), \end{aligned} \quad (5c)$$

From Eq. (5a), it can be seen that  $\boldsymbol{\psi}_0$  is independent of  $\boldsymbol{\Omega}$  (i.e., it is isotropic). Re-arranging Eq. (5b) as follows:

$$\psi_1(\mathbf{r}, \boldsymbol{\Omega}, t) = \frac{1}{4\pi} \Psi_1(\mathbf{r}, t) - \frac{1}{\Sigma(\mathbf{r})} \boldsymbol{\Omega} \cdot \nabla \psi_0(\mathbf{r}, \boldsymbol{\Omega}, t), \quad (6)$$

and substituting into Eq. (5c), the following equation is obtained:

$$\begin{aligned} \frac{1}{4\pi v} \frac{\partial}{\partial t} \Psi_0(\mathbf{r}, t) + \frac{1}{4\pi} \boldsymbol{\Omega} \cdot \nabla \left[ \Psi_1(\mathbf{r}, t) - \frac{1}{\Sigma(\mathbf{r})} \boldsymbol{\Omega} \cdot \nabla \Psi_0(\mathbf{r}, t) \right] + \Sigma(\mathbf{r})\psi_2(\mathbf{r}, \boldsymbol{\Omega}, t) \\ + \frac{\Sigma_a(\mathbf{r}) - v\Sigma_f(\mathbf{r})}{4\pi} \Psi_0(\mathbf{r}, t) - \frac{\Sigma(\mathbf{r})}{4\pi} \Psi_2(\mathbf{r}, t) = \frac{1}{4\pi} q(\mathbf{r}, t). \end{aligned} \quad (7)$$

Integrating Eq. (7) over  $\boldsymbol{\Omega}$  and noticing that

$$\oint \boldsymbol{\Omega} d\boldsymbol{\Omega} = 0$$

this equation becomes:

$$\frac{1}{v} \frac{\partial}{\partial t} \Psi_0(\mathbf{r}, t) - \oint \boldsymbol{\Omega} \cdot \nabla \frac{1}{\Sigma(\mathbf{r})} \boldsymbol{\Omega} \cdot \nabla \Psi_0(\mathbf{r}, t) d\boldsymbol{\Omega} + [\Sigma_a(\mathbf{r}) - v\Sigma_f(\mathbf{r})] \Psi_0(\mathbf{r}, t) = q(\mathbf{r}, t). \quad (8)$$

The second term in the l.h.s. in Eq. (7) can be written as:

$$\frac{1}{4\pi} \oint \boldsymbol{\Omega} \cdot \nabla \frac{1}{\Sigma(\mathbf{r})} \boldsymbol{\Omega} \cdot \nabla \Psi_0(\mathbf{r}, t) d\boldsymbol{\Omega} = \nabla \frac{1}{3\Sigma(\mathbf{r})} \cdot \nabla \Psi_0(\mathbf{r}, t). \quad (9)$$

Using Eq. (9) in Eq. (8), the following equation is obtained:

$$\frac{1}{v} \frac{\partial}{\partial t} \Psi_0(\mathbf{r}, t) - \nabla D(\mathbf{r}) \cdot \nabla \Psi_0(\mathbf{r}, t) + [\Sigma_a(\mathbf{r}) - v\Sigma_f(\mathbf{r})] \Psi_0(\mathbf{r}, t) = q(\mathbf{r}, t), \quad (10)$$

which is the well-known diffusion equation, where  $D(\mathbf{r}) = 1/3\Sigma(\mathbf{r})$  is the diffusion coefficient.

Equation (10) proves that the diffusion equation stems from a first-order **asymptotic** expansion of the linear transport equation, provided that the scaling in Eqs. (3) are physically meaningful.

Although it is generally known that in several cases diffusion theory offers a convenient approximation of linear transport problems, there are conditions for which the first-order approximation is not sufficient and/or the scaling in Eqs. (3) is not suitable. Typically, the diffusion model is inaccurate in the description of particle field:

- close to the external boundaries,
- in the presence of strong sources and absorbers,
- in the presence of strong cross section variations,
- when simulating strong excursions of source terms, and
- when considering relevant anisotropic scattering effects.

### 3. DERIVATION OF THE TRANSPORT-DRIVEN DIFFUSION METHOD

In the following, the transport-driven diffusion model is derived from LBE using a multiple collision approach (Section 3.1) and the solution of the residue is discussed, explaining how the considerations in Section 2 makes diffusion theory more suitable in a TDD framework than when used for the overall simplification of the original LBE.

#### 3.1 Formulation of the transport equation in the multiple collision fashion

The solution of Eq. (1) is decomposed in terms accounting for the contributions of different numbers of collisions, i.e.:

$$\psi(\mathbf{r}, \boldsymbol{\Omega}, t) = \psi^{[1]}(\mathbf{r}, \boldsymbol{\Omega}, t) + \psi^{[2]}(\mathbf{r}, \boldsymbol{\Omega}, t) + \psi^{[3]}(\mathbf{r}, \boldsymbol{\Omega}, t) + \dots = \sum_{j=1}^{\infty} \psi^{[j]}(\mathbf{r}, \boldsymbol{\Omega}, t), \quad (11)$$

where  $j$  is the collision order (e.g.,  $j=1$ : uncollided;  $j=2$ : first collision;  $j=3$ : second collision). The equation for the uncollided component reads:

$$\left[ \frac{1}{v} \frac{\partial}{\partial t} + \boldsymbol{\Omega} \cdot \boldsymbol{\nabla} + \Sigma(\mathbf{r}) \right] \psi^{[1]}(\mathbf{r}, \boldsymbol{\Omega}, t) = \frac{1}{4\pi} q(\mathbf{r}, t), \quad (12)$$

whereas for  $j \geq 1$  the following equation applies:

$$\left[ \frac{1}{v} \frac{\partial}{\partial t} + \boldsymbol{\Omega} \cdot \boldsymbol{\nabla} + \Sigma(\mathbf{r}) \right] \psi^{[j]}(\mathbf{r}, \boldsymbol{\Omega}, t) = \frac{\Sigma_s(\mathbf{r}) + v\Sigma_f(\mathbf{r})}{4\pi} \oint \psi^{[j-1]}(\mathbf{r}, \boldsymbol{\Omega}', t) d\boldsymbol{\Omega}'. \quad (13)$$

For each collision, the propagation of particles along different directions is decoupled and the angle  $\boldsymbol{\Omega}$  simply becomes a parameter and not an independent variable, i.e.:

$$\psi^{[j]}(\mathbf{r}, \boldsymbol{\Omega}, t) = \psi_{\boldsymbol{\Omega}}^{[j]}(\mathbf{r}, t), \quad (14)$$

and the initially integro-differential equation (see Eq. (1)) turns into a partial differential equation, i.e.:

$$\begin{aligned} \left[ \frac{1}{v} \frac{\partial}{\partial t} + \boldsymbol{\Omega} \cdot \boldsymbol{\nabla} + \Sigma(\mathbf{r}) \right] \psi_{\boldsymbol{\Omega}}^{[1]}(\mathbf{r}, t) &= q_{\boldsymbol{\Omega}}^{[0]}(\mathbf{r}, t), \\ \left[ \frac{1}{v} \frac{\partial}{\partial t} + \boldsymbol{\Omega} \cdot \boldsymbol{\nabla} + \Sigma(\mathbf{r}) \right] \psi_{\boldsymbol{\Omega}}^{[2]}(\mathbf{r}, t) &= q_{\boldsymbol{\Omega}}^{[1]}(\mathbf{r}, t), \\ &\vdots \\ \left[ \frac{1}{v} \frac{\partial}{\partial t} + \boldsymbol{\Omega} \cdot \boldsymbol{\nabla} + \Sigma(\mathbf{r}) \right] \psi_{\boldsymbol{\Omega}}^{[j]}(\mathbf{r}, t) &= q_{\boldsymbol{\Omega}}^{[j-1]}(\mathbf{r}, t), \\ &\vdots \end{aligned} \quad (15)$$

where the source terms are defined as:

$$q_{\boldsymbol{\Omega}}^{[j=0]}(\mathbf{r}, t) = \frac{1}{4\pi} q(\mathbf{r}, t) \quad (16)$$

and:

$$q_{\boldsymbol{\Omega}}^{[j]}(\mathbf{r}, t) = \frac{\Sigma_s(\mathbf{r}) + v\Sigma_f(\mathbf{r})}{4\pi} \oint \psi^{[j-1]}(\mathbf{r}, \boldsymbol{\Omega}', t) d\boldsymbol{\Omega}' \quad \text{for } j \geq 1. \quad (17)$$

The initial and boundary conditions for the uncollided particles are:

$$\begin{aligned}\psi^{[j=1]}(\mathbf{r}_s, \boldsymbol{\Omega}, t) &= f(\mathbf{r}_s, \boldsymbol{\Omega}, t) \quad \text{for } \boldsymbol{\Omega} \cdot \mathbf{n}_s < 0, \\ \psi^{[j=1]}(\mathbf{r}, \boldsymbol{\Omega}, t = 0) &= \psi_0(\mathbf{r}, \boldsymbol{\Omega}),\end{aligned}\tag{18}$$

whereas for successive generations these conditions become:

$$\begin{aligned}\psi^{[j>1]}(\mathbf{r}_s, \boldsymbol{\Omega}, t) &= 0 \quad \text{for } \boldsymbol{\Omega} \cdot \mathbf{n}_s < 0, \\ \psi^{[j>1]}(\mathbf{r}, \boldsymbol{\Omega}, t = 0) &= 0.\end{aligned}\tag{19}$$

The price to pay for the simplification of the mathematical nature of the equations (from integro-differential as is the original full transport equation to purely differential) is that a set of infinite equations needs to be solved. Hence, a truncation becomes necessary in order to make the approach numerically manageable, i.e.:

$$\psi(\mathbf{r}, \boldsymbol{\Omega}, t) \approx \sum_{j=1}^T \psi^{[j]}(\mathbf{r}, \boldsymbol{\Omega}, t),\tag{20}$$

where  $T$  is the truncation order. This assumption is equivalent to disregard the contributions of collisions with orders higher than  $T$ .

In the past, solving the linear transport equation directly via a multiple collision procedure recalling the Neumann approach to solve integral equations was attempted and interesting theoretical investigations were published (e.g., Ganapol and Grossman, 1973; Ganapol, 1982a, 1982b, 1985, 1999). Depending on the medium properties, a different number of collisions have to be considered to achieve the same accuracy. In case of a system with a small number of secondaries per collisions (i.e.,  $\Sigma_s/\Sigma \ll 1$ ), the convergence of the series is rather fast and the multiple collision approach can be a feasible solution strategy. When dealing with highly scattering media, the truncation order has to be consistently increased, with a considerable limitation for computational performances.

### 3.2 Transport-driven diffusion

In the recent past, a different approach was proposed, namely the transport-driven diffusion (Picca and

Furfaro, 2014). The idea is to start from the multiple collision formulation of the LBE and introduce a residue after truncation, i.e.:

$$\psi(\mathbf{r}, \boldsymbol{\Omega}, t) = \sum_{j=1}^T \psi^{[j]}(\mathbf{r}, \boldsymbol{\Omega}, t) + z(\mathbf{r}, \boldsymbol{\Omega}, t). \quad (21)$$

The equation for the residue is written as:

$$\left[ \frac{1}{v} \frac{\partial}{\partial t} + \boldsymbol{\Omega} \cdot \boldsymbol{\nabla} + \Sigma(\mathbf{r}) \right] z(\mathbf{r}, \boldsymbol{\Omega}, t) = \frac{\Sigma_s(\mathbf{r}) + v\Sigma_f(\mathbf{r})}{4\pi} \left[ \oint z(\mathbf{r}, \boldsymbol{\Omega}', t) d\boldsymbol{\Omega}' + \oint \psi^{[T]}(\mathbf{r}, \boldsymbol{\Omega}', t) d\boldsymbol{\Omega}' \right]. \quad (22)$$

The above equation retains the same mathematical nature as the original linear Boltzmann problem in Eq. (1). Based on physical considerations, Picca and Furfaro argued in (2014) that the residue can be approached by a simplified approach, such as the diffusion equation. Their analysis proves that this intuition is fundamentally correct, presenting results that show how the accuracy is considerably improved with respect to the classical diffusion approximation of Eq. (1). Expanding the residue in Eq. (13) as in Eqs. (4), the diffusion equation for the residue can be finally written as:

$$\frac{1}{v} \frac{\partial}{\partial t} Z(\mathbf{r}, t) + \boldsymbol{\nabla} \cdot \mathbf{D}(\mathbf{r}) \boldsymbol{\nabla} Z(\mathbf{r}, t) + [\Sigma_a(\mathbf{r}) - v\Sigma_f(\mathbf{r})] Z(\mathbf{r}, t) = \Psi^{[T]}(\mathbf{r}, t), \quad (23a)$$

where

$$Z(\mathbf{r}, t) = \oint z(\mathbf{r}, \boldsymbol{\Omega}, t) d\boldsymbol{\Omega}, \quad (23b)$$

$$\Psi^{[T]}(\mathbf{r}, t) = \oint \psi^{[T]}(\mathbf{r}, \boldsymbol{\Omega}, t) d\boldsymbol{\Omega}, \quad (23c)$$

and the diffusion problem for  $Z(\mathbf{r}, t)$  is complemented with standard radiative boundary conditions, assuming an extrapolation length equal to 0.71 mfp. We can define an order of the TDD approximation, based on the collision order  $T$  (i.e.  $\text{TDD}_T$ )

### 3.3 Analysis of the residue equation

This section discusses in detail why the diffusion model is more suitable for the description of the residue than for the solution of the general problem. For this purpose, a function  $\alpha$ , defined as the ratio of the particle density after  $T$  collisions and the residue, is introduced:

$$\alpha_T(\mathbf{r}, t) = \frac{\Psi^{[T]}(\mathbf{r}, t)}{Z(\mathbf{r}, t)}. \quad (24)$$

Numerical results show that the difference between the spatial distribution of  $\Psi^{[T]}$  and  $Z$  narrows when increasing the order of collision  $j$ , i.e. the distribution tends to stabilize when sufficiently “far” (in terms of collisions) from the external source. Intuitively, this is the result of the first generations being strongly influenced by the external driving term and, after several generations, the spatial distribution being determined only by the physical and geometrical properties of the medium. The establishment of an asymptotic behavior in general may take several generations due to the migration process, especially in optically thick systems. As a result of this,  $\alpha$  tends to a constant when increasing the collision order **in diffusion-dominated regions (e.g., far away from interfaces and boundaries)**. **If such condition is met, the residue can be written in terms of  $\Psi^{[T]}$ , explicitly:**

$$Z(\mathbf{r}, t) \approx \frac{1}{\bar{\alpha}} \Psi^{[T]}(\mathbf{r}, t), \quad (25)$$

where  $\bar{\alpha}$  is an appropriate constant value.

Using Eq. (24) in Eq. (23a), the equation for the residue becomes:

$$\left[ \frac{1}{v} \frac{\partial}{\partial t} + \boldsymbol{\Omega} \cdot \boldsymbol{\nabla} + \Sigma(\mathbf{r}) \right] z(\mathbf{r}, \boldsymbol{\Omega}, t) = (1 + \alpha_T(\mathbf{r}, t)) \frac{\Sigma_s(\mathbf{r}) + v\Sigma_f(\mathbf{r})}{4\pi} Z(\mathbf{r}, t), \quad (26)$$

which is in the form of a source-free LTE with a fictitiously increased number of secondaries per collision:

$$\Sigma_s(\mathbf{r}) + v\Sigma_f(\mathbf{r}) = c\Sigma(\mathbf{r}) \rightarrow c\Sigma^*(\mathbf{r}) = (1 + \alpha_T(\mathbf{r}, t))c\Sigma(\mathbf{r}). \quad (27)$$

It is clear that in general the applicability of the scaling in Eq. (3) better suits the residue equation in Eq. (13) than the initial transport equation in Eq. (1) as:

- the collisional component is larger than in the original problem;
- there is no external source term.

Note that in the case of a strong fission contribution, higher orders of TDD are needed to achieve the same accuracy, as it is discussed in the result section.

In practical applications,  $\alpha_T$  cannot be evaluated as it requires the **full solution of the LBE**, Eqs. (1). A potential surrogate of  $\alpha_T$  which is more easily available during computation, is the ratio between the solutions of the last two collisions:

$$\gamma_T(\mathbf{r}, t) = \frac{\Psi^{[T+1]}(\mathbf{r}, t)}{\Psi^{[T]}(\mathbf{r}, t)} \quad (28)$$

In order for  $\alpha_T$  to **show the asymptotic behavior described above**, the value of  $\gamma_T$  is expected to become spatially constant (i.e., at convergence, the shape of the next generation resembles the previous one) and its value is related to the inverse of the number of secondaries per collision.

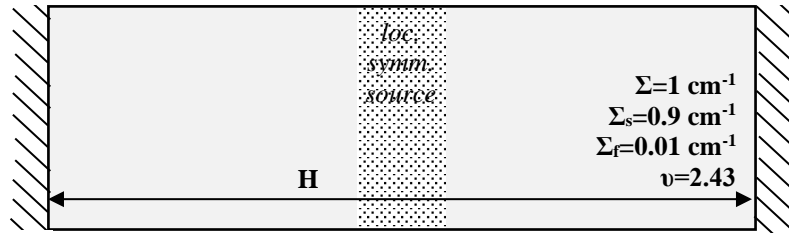
## 4. RESULTS

### 4.1 Test cases: problem set up and computational parameters

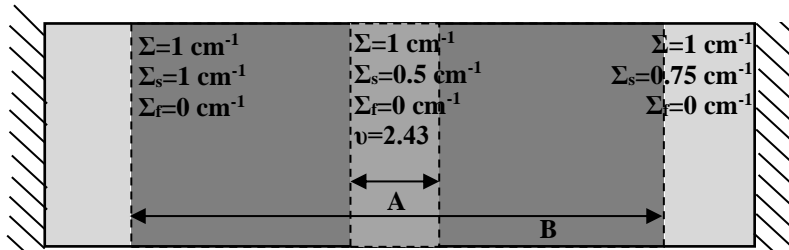
The concept presented in previous sections is now tested in several problems. Figure 1 presents a summary of the different configurations analyzed. For demonstration purposes, a 1D system is considered, as the multidimensionality of the problem is not expected to influence the generality of the findings. Two configurations are considered: a homogeneous medium and a heterogeneous system, more representative of an accelerator-driven system (ADS). Table 1 presents the set of test cases considered.

The solution adopted as reference for the comparisons is evaluated solving the transport equation with standard  $S_N$  (Lewis and Miller, 1993). Ten discrete directions are used for the steady-state solution and 100 directions for the time-dependent cases, to cope with ray effects. Finite volumes are used for space discretization (400 meshes) and Implicit Euler finite differences for the time variable (time mesh 0.05 mft, defined as the time a particle takes to cover 1 mean free path). The scattering term is treated via source iterations with convergence tolerance on the L-infinity norm of the flux set to 1e-6. The diffusion equation is solved using finite volumes for space and finite differences for the time variable using the same spatial and time discretizations used for the solution of the transport equations at each

collision order. In Section 4.2 and Section 4.3 the steady-state and the time-dependent comparisons are presented.



a) homogeneous medium



b) heterogeneous medium

Figure 1. Description of the configurations considered. Additional data:  $\nu=1$  cm/s;  $A=1/16$  H;

$$B=3/4 H.$$

Table 1. Summary of the test cases considered.

| Case ID | Geometry      | H [cm] | $k_{\text{eff}}$<br>(adjusting $\nu$ ) | Source distribution               | Objective of the test case(s)            |
|---------|---------------|--------|--|-----------------------------------|--|
| A       | homogeneous   | 2      | 0                                      | uniform,<br>constant in<br>time   | testing effect<br>of dimensions          |
| B       |               | 10     |  |                                   |  |
| C       |               | 20     |  |                                   |  |
| D       |               | 100    |  |                                   |  |
| E       |               | 20     | 0.5                                    |                                   | reference case<br>for steady-<br>state   |
| F       |               |        | 0.9                                    |                                   |  |
| G1      | heterogeneous | 20     | 0.97                                   | localized,<br>constant in<br>time | reference case<br>for time-<br>dependent |
| G2      |               |        |  | localized,<br>1 mft pulse         |  |

## 4.2 Steady-state solutions

Figures 2 and 3 present the steady-state solution for the homogeneous cases to study the effect of different system dimensions. It can be seen that the convergence of the multiple collision approach requires a larger value of  $T$  for optically larger systems (top graphs), while the behavior of the indicators  $\alpha_T$  and  $\gamma_T$  tends to flatten with increasing collision contribution, thus indicating that TDD works better than diffusion in reproducing the reference solution. On the computational side, it must be pointed out that  $\gamma_T$  can be easily computed during the code execution, while the evaluation of  $\alpha_T$  requires that the solution is known. Consequently,  $\gamma_T$  can be used in practical applications as a surrogate of  $\alpha_T$ .

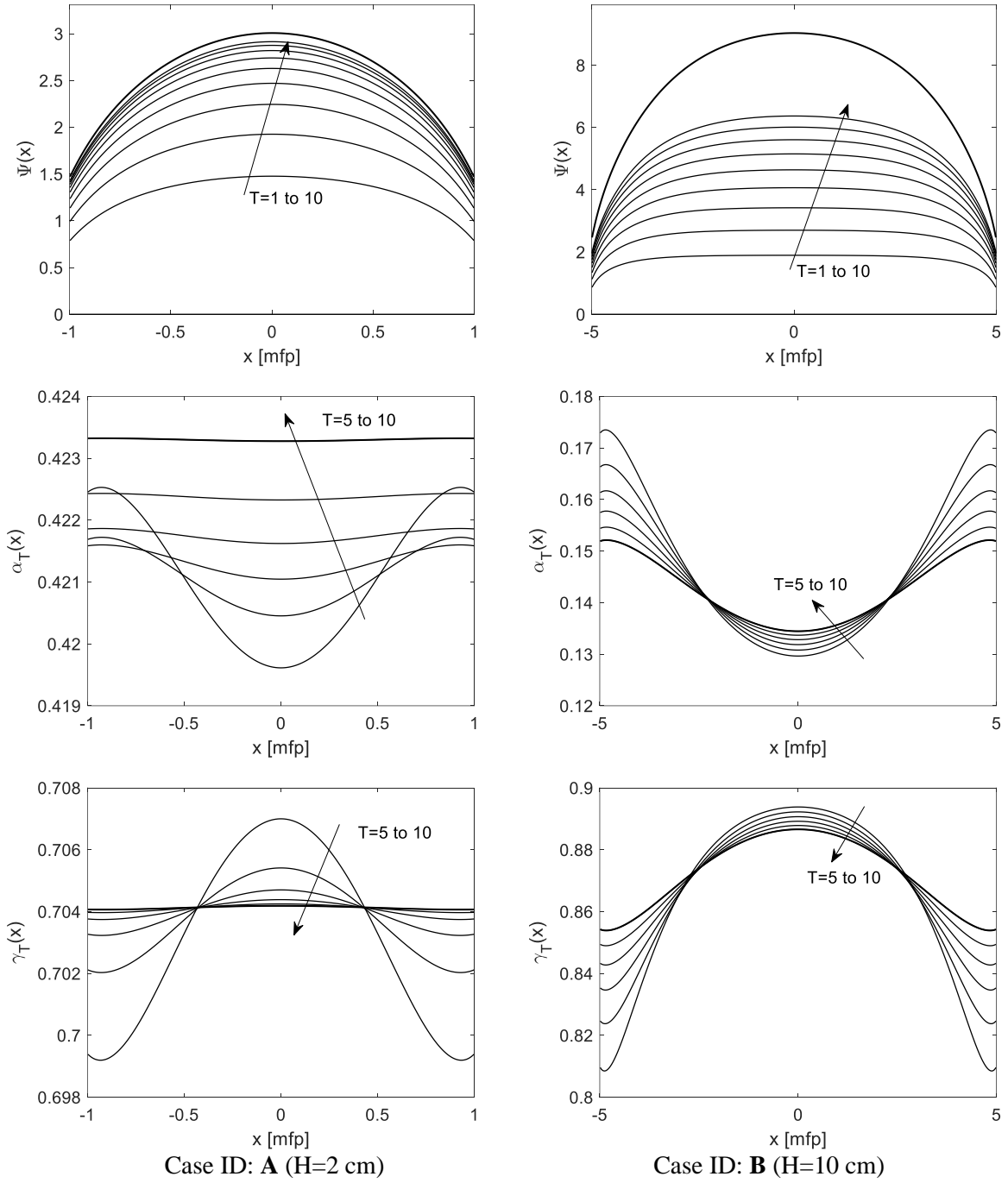
In Figure 4 the solution for the same homogeneous problem with fixed dimension  $H=20$  is reported, introducing a fission emission contribution, leading to two different values of  $k_{\text{eff}}$ . Clearly, the presence of the fission phenomenon leads to the requirement of a larger number of collisional terms, while the behavior of the indicators  $\alpha_T$  and  $\gamma_T$  is consistent with the previous cases.

Figure 5 presents the results for a heterogeneous configuration, simulating a source-driven system situation. The heterogeneity is clearly affecting the spatial flux distribution and the value of  $k_{\text{eff}}$  impacts on the order of collision expansion  $T$ .

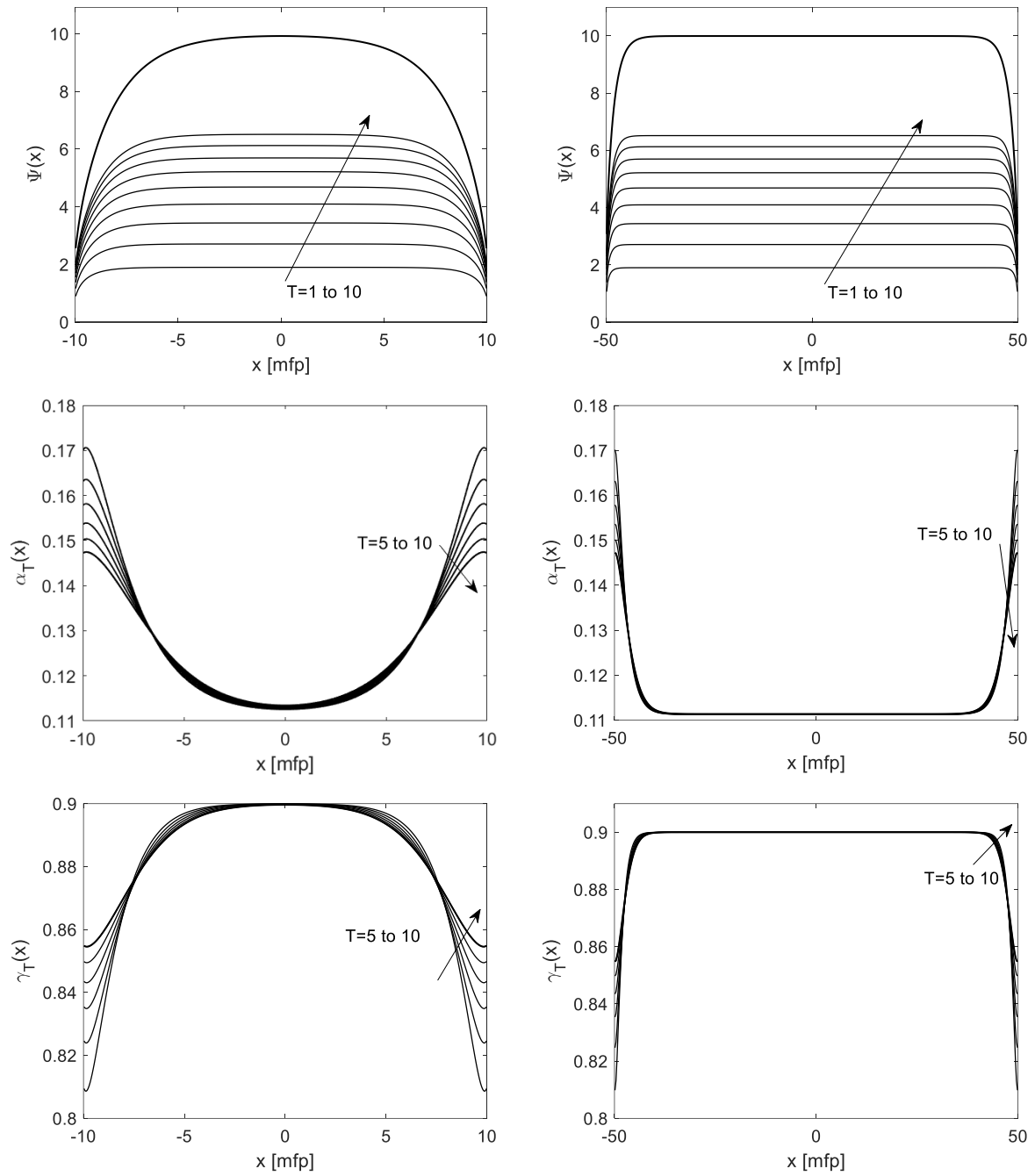
The various solution approaches for the configuration G1 are compared in Figure 6, varying the collision order  $T$  adopted. It appears that, in general, TDD outperforms both the diffusion and the multiple collision solutions, and the efficacy of TDD improves as the truncation order increases.

Table 2 reports the computational times, normalized to the reference, for case G1, to highlight the significant advantage of TDD as compared to the reference transport solution. Whilst the diffusive approach turns out to be more computationally efficient, as expected, it is far less accurate (see Figure 6) compared to TDD. TDD also proves to be very competitive compared to the reference solution, even at high order (e.g., the computational time for TDD<sub>200</sub> is less than a third of that for the full transport inversion).

The trend of  $\gamma_T$  as a function of the parameter  $T$  (Figures 2 through 5), as well as the general trend in the reduction of the error when increasing  $T$  (Figure 6), suggest the possibility to automate the selection of the order  $T$  to target a certain accuracy, which will be the object of further investigations.



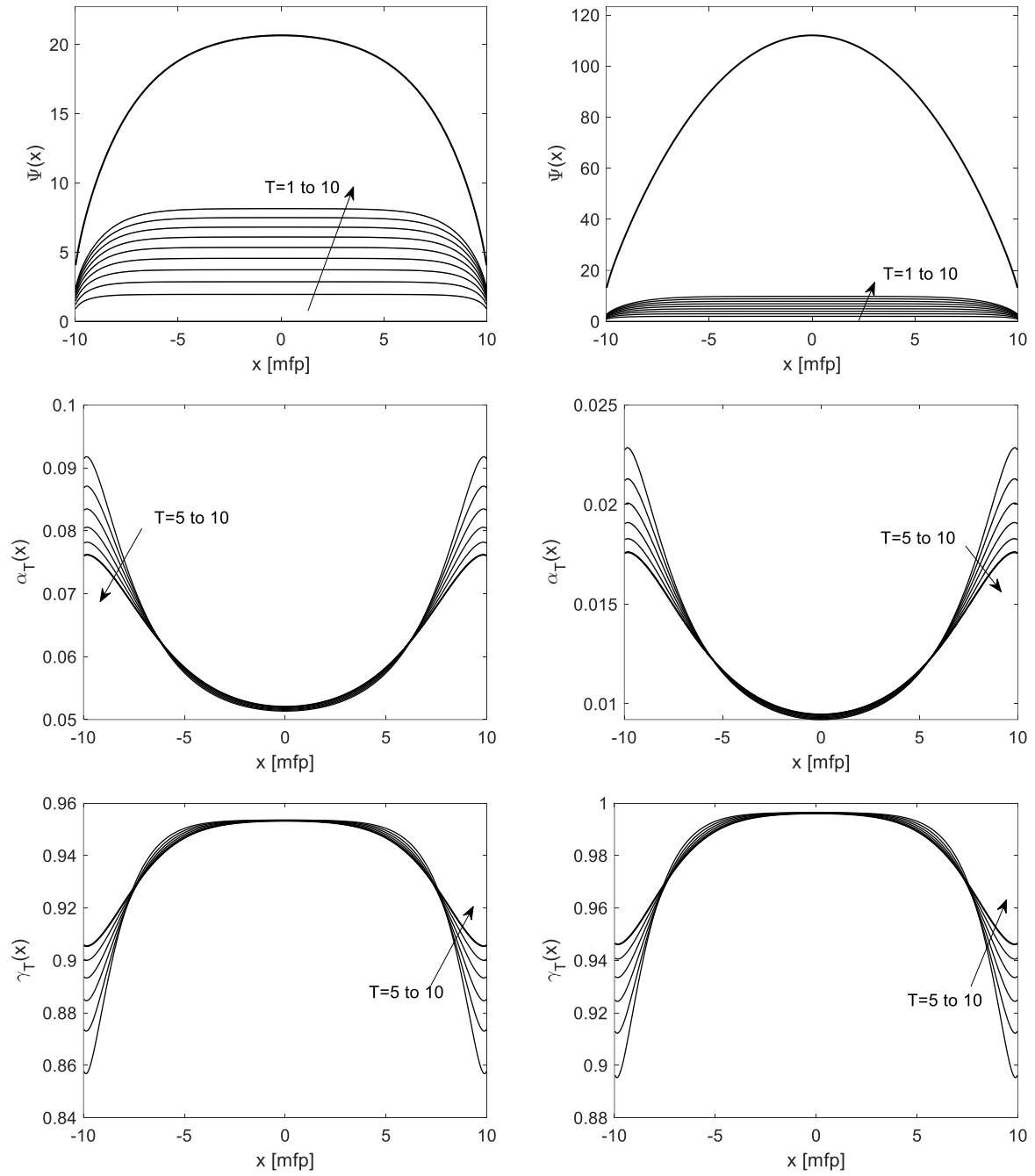
**Figure 2. Total flux  $\Psi$ ,  $\alpha_T$  and  $\gamma_T$  for cases A and B. In the top graphs the multiple collision solution is also presented.**



Case ID: **C** (H=20 cm)

Case ID: **D** (H=100 cm)

**Figure 3. Total flux  $\Psi$ ,  $\alpha_T$  and  $\gamma_T$  for cases C and D. In the top graphs the multiple collision solution is also presented.**



Case ID: **E** (H=20 cm,  $k_{\text{eff}}=0.5$ )

Case ID: **F** (H=20 cm,  $k_{\text{eff}}=0.9$ )

**Figure 4. Total flux  $\Psi$ ,  $\alpha_T$  and  $\gamma_T$  for cases E and F. In the top graphs the multiple collision solution is also presented.**

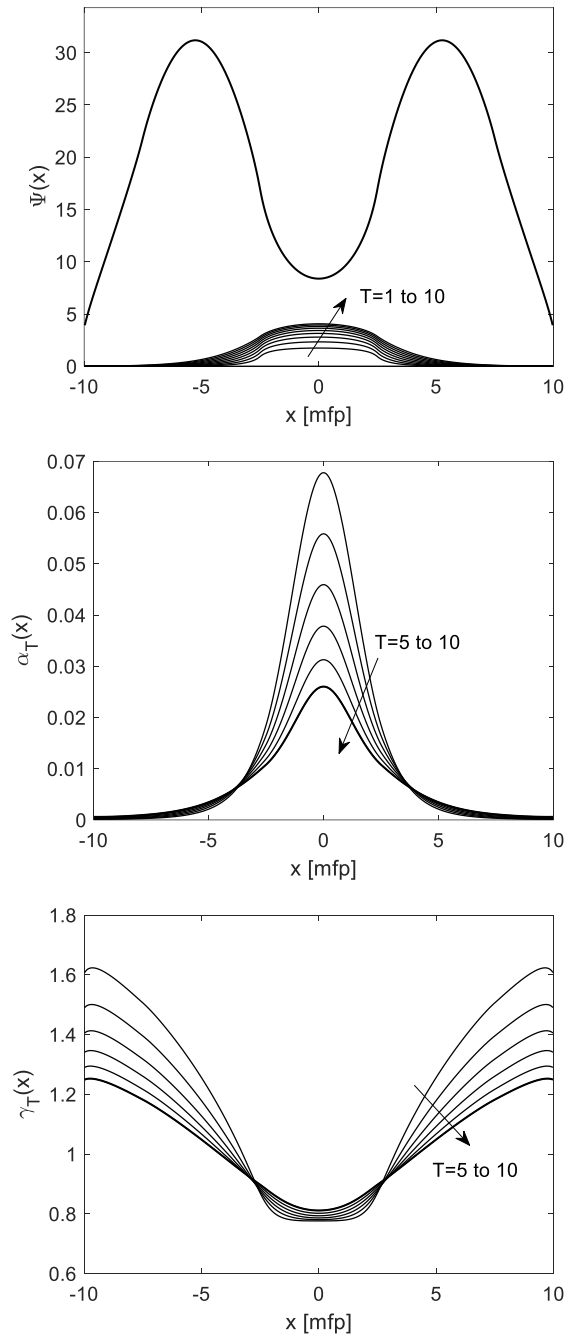


**Figure 5. Total flux  $\Psi$ ,  $\alpha_T$  and  $\gamma_T$  for case G1 ( $H=20$  cm,  $k_{\text{eff}}=0.97$ , localized source). In the top graphs the multiple collision solution is also presented.**

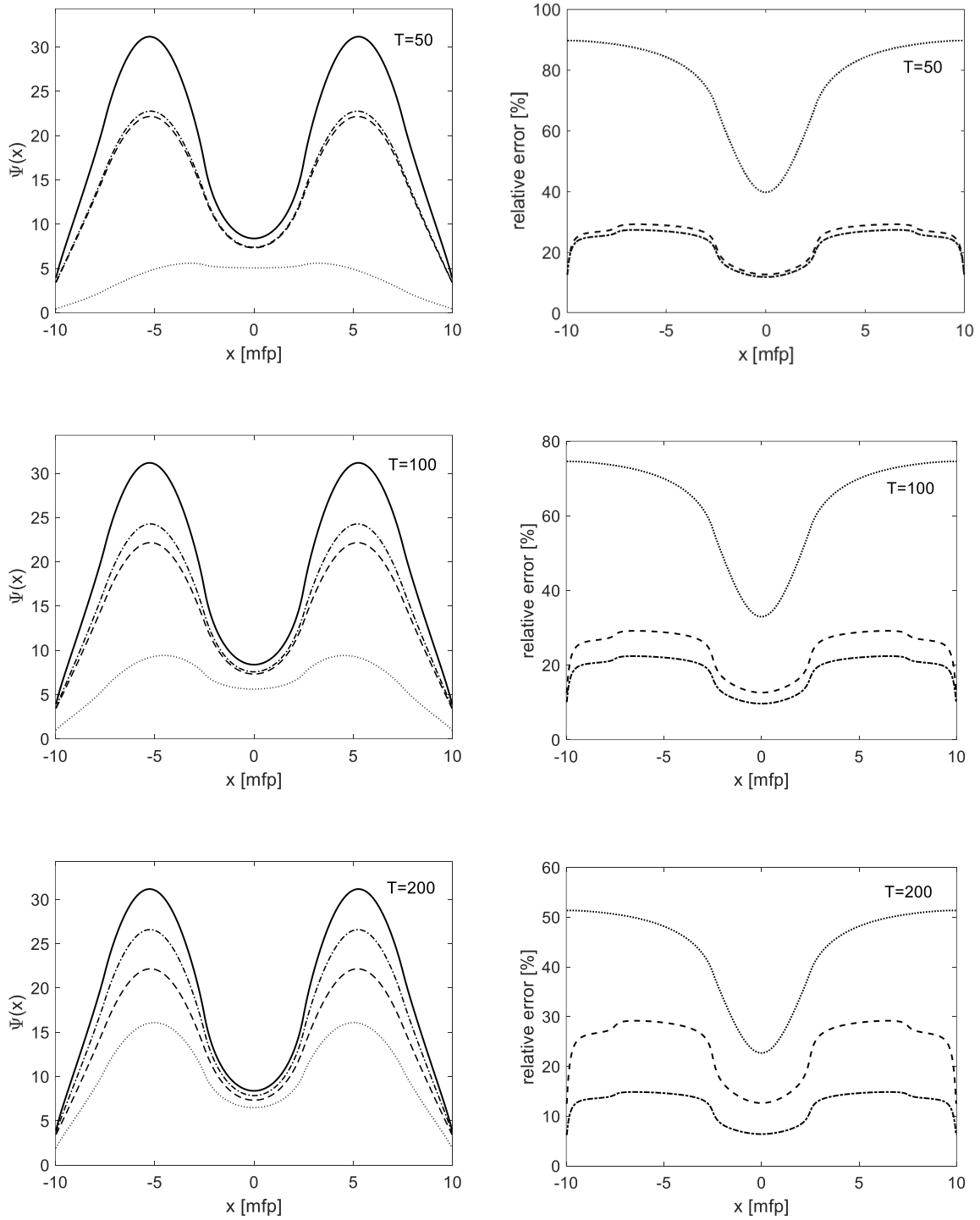


**Figure 6. Comparison of various solution techniques for the steady-state problem G1 ( $H=20$  cm,  $k_{\text{eff}}=0.97$ , localized source). Solid line: reference transport; dotted line: diffusion; dashed line: multiple collision; dash-dotted line: TDD<sub>T</sub>. Left: flux distributions; right: percentage relative error with respect to the reference.**

**Table 2. Comparison of computational performances for steady-state case. The computational time in the table is normalised to the reference  $S_N$  transport solution.**

| <b>solution method</b>            | <b>normalized computational time</b> |
|-----------------------------------|--------------------------------------|
| <b>Diffusion</b>                  | 0.03                                 |
| <b>multiple collision (T=50)</b>  | 0.04                                 |
| <b>TDD<sub>50</sub></b>           | 0.07                                 |
| <b>multiple collision (T=100)</b> | 0.08                                 |
| <b>TDD<sub>100</sub></b>          | 0.11                                 |
| <b>multiple collision (T=200)</b> | 0.23                                 |
| <b>TDD<sub>200</sub></b>          | 0.26                                 |

### 4.3 Time-dependent solution

In this section the the time-dependent case G2 is studied. The system is injected with a source pulse of duration 1 mft. **The details on the location and characteristics of the source are provided in Figure 1a.**

In Figure 7 the error associated to the solution approaches as compared to the reference are evaluated in the center of the system and presented as a function of time, assuming different values of  $T$ , in order to highlight the significant advantage of TDD also in time-dependent situations. The graphs on the right show that a variable number of collision terms may be needed as the transient evolves, as expected from the physical point of view as the contribution of collisions increases over time. In Figure 8 the same set of results are plotted in a position within the fissile region. As can be seen, the error of the diffusion solution becomes more relevant since the diffusion model cannot account for the finite velocity of the particles moving off the source. These effects are enhances moving farther from the system center, as visible in Figure 9.

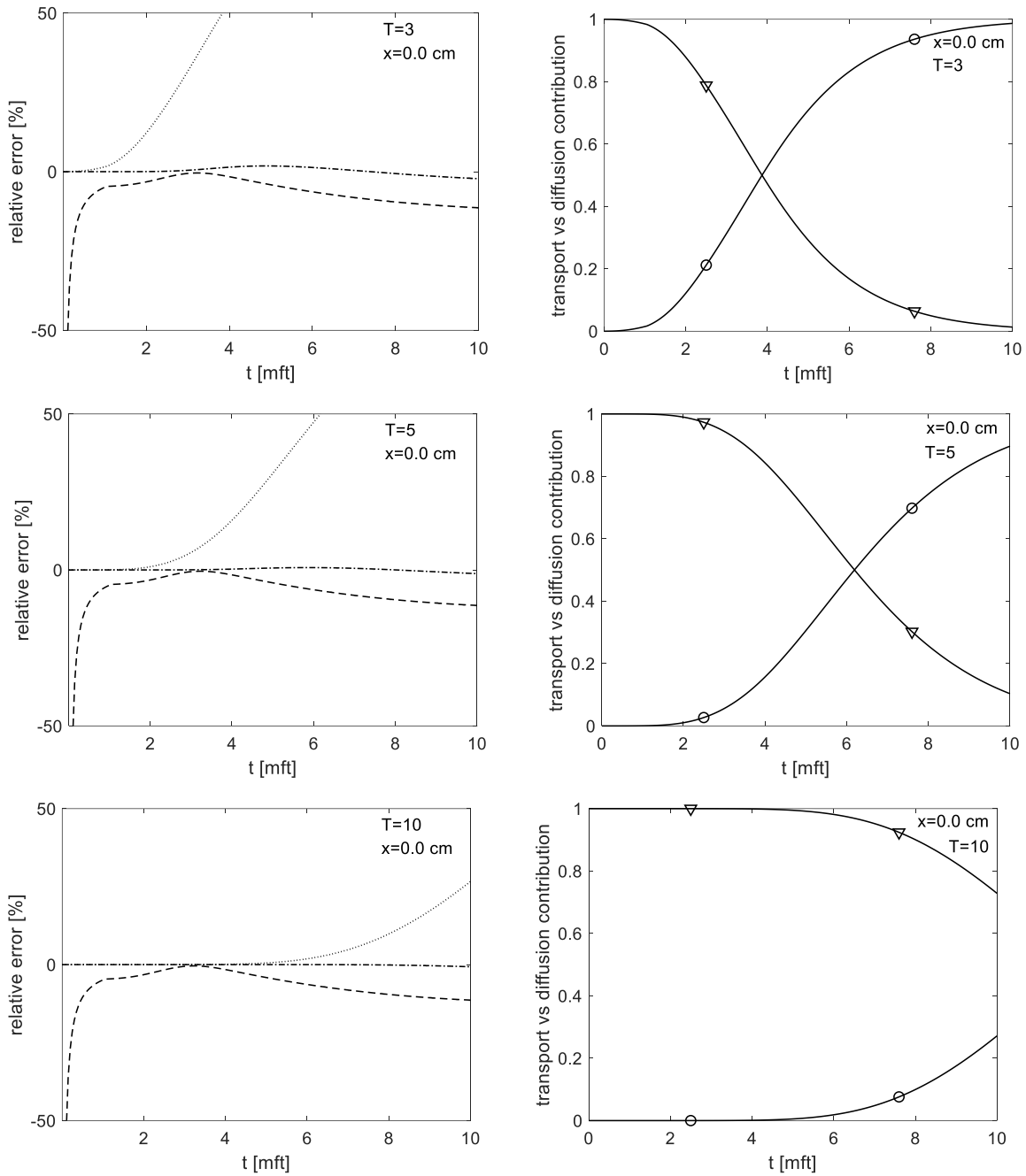
The convergence pattern of TDD with increasing values of  $T$  is reported in Figure 10. It is interesting to see that TDD error is relatively large at the beginning of the transient because of the diffusion contribution and its propagation velocity. As time progresses, the TDD error reduces drastically, the reduction being faster for larger values of  $T$ . It is worth noting that diffusion is always far more inaccurate at the beginning of the transient, whilst multi collision is relatively accurate at the

beginning of the transient before becoming largely inaccurate when the error due to truncation becomes significant (i.e. multi-collided particles becomes more relevant after several collision time in the transient).

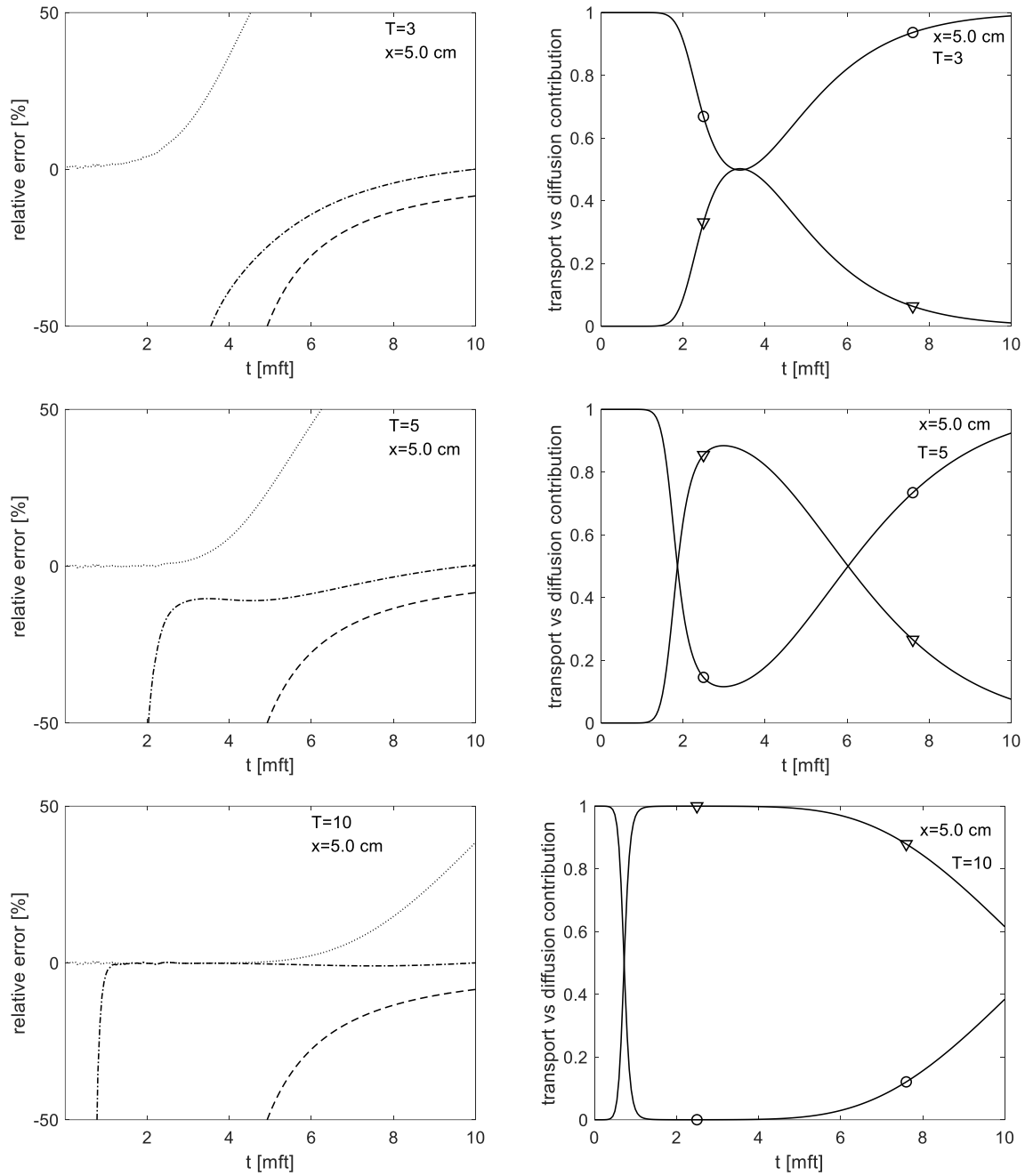
At last, Figure 11 shows the spatial behavior of the indicator  $\gamma_T$  at two different time instants during the source transient. The flattening of the shape of  $\gamma_T$  is clearly visible, although it is not homogeneous across the transient (see effect of  $T$  on the error as a function of time in Figure 10).

Table 3 evidences the limits of the TDD approach for time-dependent problems, as a high value of  $T$  leads to a penalization of the computational burden. This is due to the fact that for the reference solution source iteration at later times in the transients can require less than  $T$  iterations, making TDD less computationally advantageous. However, with small values of  $T$ , the TDD algorithm is more efficient than a direct solution (see Table 3) and more accurate than multiple collision and diffusion (see Figure 10). Whilst additional investigations are needed, it is expected that the computational performance of higher order TDD can be improved by introducing a variable order TDD, with  $T$  decreasing as time passes and the transport effect becomes less relevant.

Whilst Figure 11 show how the absolute value of  $\gamma_T$  reduces and the curve flattens as  $T$  increases, the adaptive selection of  $T$  based on  $\gamma_T$  remains to be explored in future work.



**Figure 7. Left: relative percentage error of TDD, transport and diffusion evaluated in the system center (inside the source region) of case G2 for different values of T; dotted line: diffusion; dashed line: multiple collision; dash-dotted line: TDD. Right: transport (triangle) and diffusion (circle) contributions in the TDD solution evaluated in the system center of case G2 for different values of T.**



**Figure 8. Left: relative percentage error of TDD, transport and diffusion evaluated at coordinate  $x=5$  cm (outside the source, in the multiplicative region) of case G2 for different values of  $T$ ; dotted line: diffusion; dashed line: multiple collision; dash-dotted line: TDD. Right: transport (triangle) and diffusion (circle) contributions in the TDD solution evaluated at coordinate  $x=5$  cm of case G2 for different values of  $T$ .**

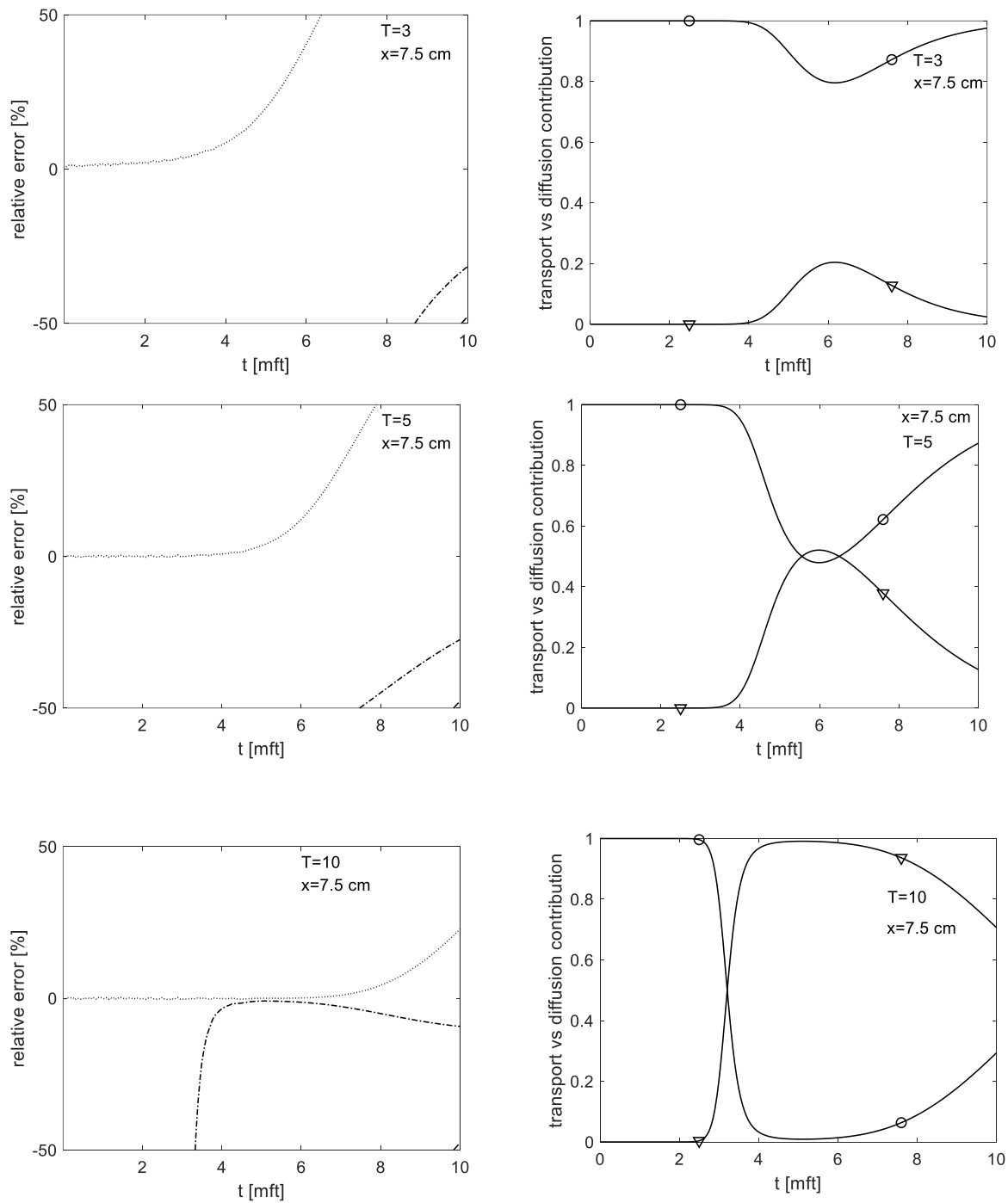


**Figure 9. Left: relative percentage error of TDD, transport and diffusion evaluated at coordinate  $x=7.5$  cm (interface between fissile material and reflector) of case G2 for different values of  $T$ ; dotted line: diffusion; dashed line: multiple collision; dash-dotted line: TDD. Right: transport (triangle) and diffusion (circle) contributions in the TDD solution evaluated at coordinate  $x=7.5$  cm of case G2 for different values of  $T$ .**

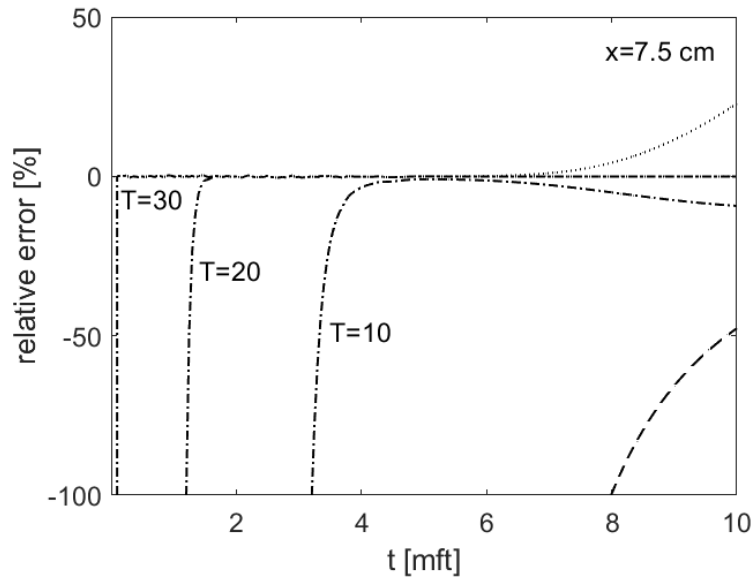


**Figure 10. Relative percentage error of  $TDD_T$  solutions of various orders at  $x=7.5$  cm (interface between fissile material and reflector) of case G2. Dashed line: multiple collision ( $T=10$ ); dash-dotted line: TDD.**

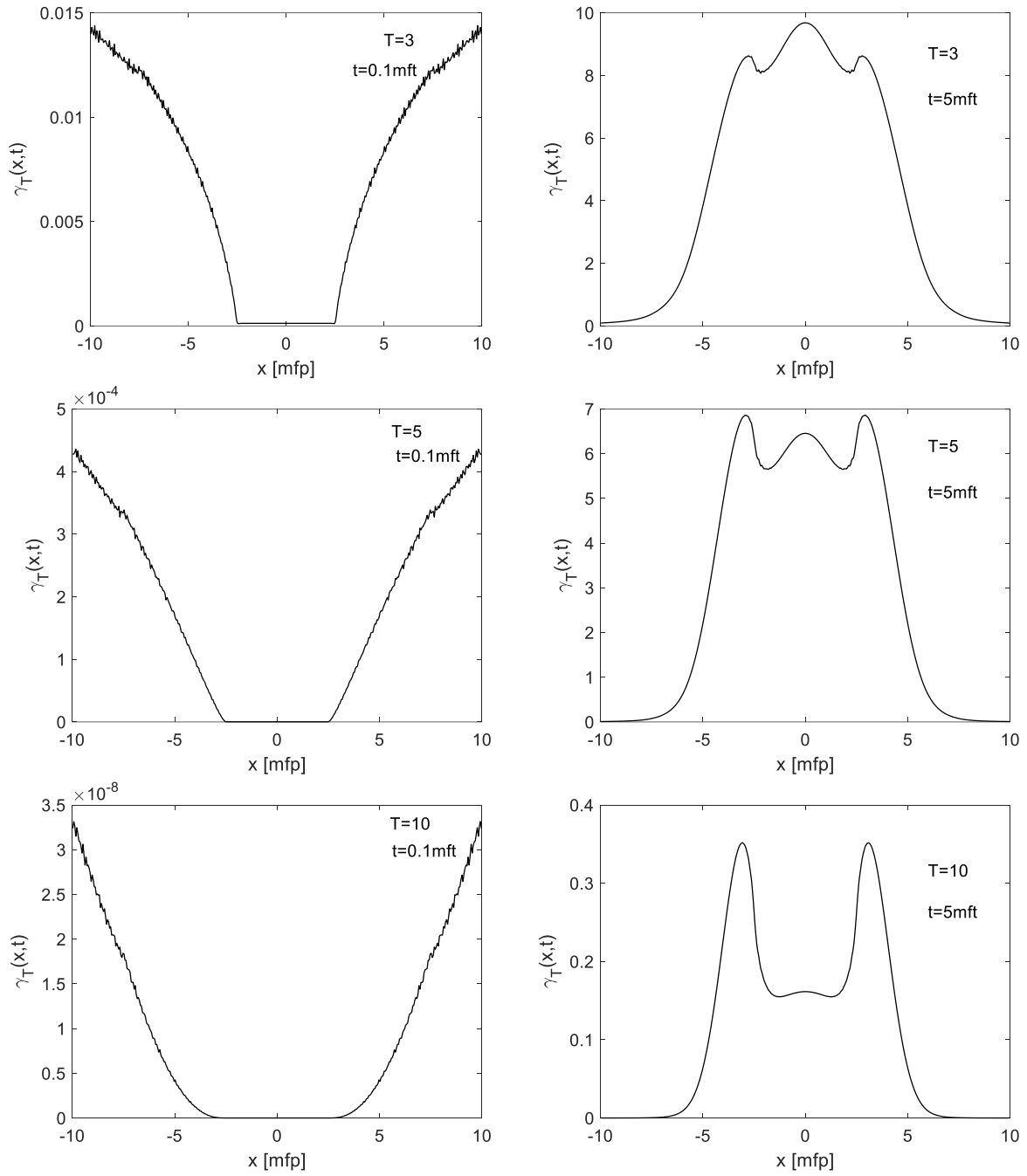


**Figure 11. Spatial behavior of  $\gamma_T$  at two instants during the source transient of case G2 for different values of  $T$ .**

**Table 3. Comparison of computational performance for the time-dependent case G2. The computational times in the table are normalised to reference  $S_N$  transport solution.**

| <b>solution method</b>           | <b>normalized computational time</b> |
|----------------------------------|--------------------------------------|
| <b>Diffusion</b>                 | 0.01                                 |
| <b>multiple collision (T=3)</b>  | 0.60                                 |
| <b>TDD<sub>3</sub></b>           | 0.61                                 |
| <b>multiple collision (T=5)</b>  | 0.95                                 |
| <b>TDD<sub>5</sub></b>           | 1.05                                 |
| <b>multiple collision (T=10)</b> | 1.65                                 |
| <b>TDD<sub>10</sub></b>          | 1.76                                 |
| <b>TDD<sub>20</sub></b>          | 3.56                                 |
| <b>TDD<sub>30</sub></b>          | 5.60                                 |

## 5. CONCLUSIONS

The foundations of the hybrid transport-driven diffusion method are presented and physically interpreted. The method is based on a combination of a transport solution accounting for various order of collisions, with a diffusion correction for the residual. The analysis presented in this paper provides an explanation of the rationale behind transport-driven diffusion, based on the observation of the evolution of the spatial distribution of each collision and on the assumptions of the diffusion model. The limitation of classical diffusion for approximating the transport equation are reviewed, presenting how modeling of the first few collisions with transport helps creating conditions for which diffusion is a suitable approximation.

The method is applied to a set of test cases in steady-state and transient conditions, comparing the transport-driven diffusion results with reference calculations, in terms of accuracy and computational effort. The advantages of the method proposed are shown using different indicators. The method proves to be advantageous with respect to a direct multiple collision approach in terms of accuracy, as it provides an efficient closure of the collision process using a diffusion estimation of the residual. Equally, TDD is also more accurate than standard diffusion, especially in time-dependent situations where the effect of the infinite propagation velocity is limited by using multi-collision transport for the first collisions. In the time-dependent case, an adaptive approach for the selection of the truncation order of TDD, e.g., based on the analysis of the trend of  $\gamma_T$ , may be required, which will be subject of future investigations.

The paper provides interesting physical insights in how neutrons propagate in scattering and multiplying media, highlighting how multiple-collided neutrons manifest a collective diffusive behavior, as compared to uncollided particles and those that have suffered a small number of collisions. TDD may thus offer a viable alternative option for the solution of transport problems.

## REFERENCES

M.L. Adams, E.W. Larsen, Fast Iterative Methods for Discrete Ordinates Particle Transport Calculations, Progress in Nuclear Energy, 40, pp. 3 – 159, 2002.

G. Bal, Transport through diffusive and non-diffusive regions, **embedded** objects, and clear layers, SIAM J. Appl. Math., 62(5), pp. 1677-1697, 2002.

G. Bal, Particle transport through scattering regions with clear layers and inclusions, J. Comp. Phys., 180(2), pp. 659-685, 2002.

G.I. Bell, S. Glasstone, Nuclear Reactor Theory, Van Nostrand, New York, 1970.

K.M. Case, P.F. Zweifel, Linear Transport Theory, Addison-Wesley, Reading, MA, 1967.

K.M. Case, Elementary solutions of the transport equation and their applications, Annals of B. Davison, Neutron Transport Theory, Oxford University Press, London, 1957.

**J.D. Densmore, "Interface Methods for Hybrid Monte Carlo-Diffusion Radiation-Transport Simulations," Ann. Nucl. Energy 33, 343 (2006).**

Physics, 9 (1960) 1-23.

B.D. Ganapol, L.M. Grossman, The collided flux method for time-dependent neutron transport. Nucl. Sci. Eng. 52 (1973) 454.

B.D. Ganapol, Time-dependent surface angular flux for a semi-infinite medium with specular reflection. Nucl. Sci. Eng. 80 (1982) 412.

B.D. Ganapol, W.L. Filippone, Time-dependent emergent intensity from an anisotropically scattering semi-infinite atmosphere, J. Quant. Spectrosc. Radiat. Transf. 27 (1982) 15.

B.D. Ganapol, Reconstruction of the time-dependent monoenergetic neutron flux from moments, J. Comp. Phys. 59 (1985) 468.

B.D. Ganapol, Homogeneous Infinite Media Time-Dependent Analytic Benchmarks for X-TM, Transport Methods Development, Technical Report, Los Alamos National Laboratory, March 1999.

**N.A. Gentile, "Implicit Monte Carlo Diffusion – An Acceleration Method for Monte Carlo Time-Dependent Radiative Transfer Simulations," J. Comp. Phys. 172, 543 (2001).**

E. Larsen, Diffusion theory as an asymptotic limit of transport theory for nearly critical systems with small mean free paths, Annals of Nuclear Energy, 7, 249-255 (1980).

E.E. Lewis, W.F. Miller, Computational Methods of Neutron Transport, American Nuclear Society, La Grange Park, Illinois, 1993.

R.V. Meghreblian, D.K. Holmes, Reactor Analysis, McGraw-Hill, 1960.

P. Picca, R. Furfaro, A hybrid method for the solution of linear Boltzmann equation. *Ann. 510 Nucl. Energy* 72:214–236, 2014.